

1 **Title**

2 **BTK operates a phospho-tyrosine switch to**
3 **regulate NLRP3 inflammasome activity**

4 **Authors**

5 Zsófia A. Bittner^a, Xiao Liu^a, Sabine Dickhöfer^a, Hubert Kalbacher^b, Karlotta Bosch^a, Liudmila
6 Andreeva^{c,d}, Ana Marcu^a, Stefan Stevanovic^a, Matthew Mangan^{e,f}, Peter Düwell^e, Marta Lovotti^e,
7 Franziska Herster^a, Markus W. Löffler^{a,g,h,i}, Sangeetha Shankar^a, Ana Tapia-Abellán^a, Olaf-Oliver
8 Wolz^{a,s}, Nadine A. Schilling^j, Jasmin Kümmerle-Deschner^k, Samuel Wagner^l, Anita Delor^m, Bodo
9 Grimbacher^{m,n,o,p,q}, Hao Wu^{c,d}, Eicke Latz^{e,r}, Alexander N. R. Weber^{a,i*}

10 **Affiliations**

11 ^a Interfaculty Institute for Cell Biology, Department of Immunology, University of Tübingen, Auf der
12 Morgenstelle 15, 72076 Tübingen, Germany

13 ^b Interfaculty Institute of Biochemistry, University of Tübingen, Hoppe-Seyler-Str. 4, 72076 Tübingen,
14 Germany

15 ^c Department of Biological Chemistry and Molecular Pharmacology, Harvard Medical School, 240
16 Longwood Avenue, C-213, Boston, MA 02115, USA

17 ^d Program in Cellular and Molecular Medicine, Boston Children's Hospital, 3 Blackfan Circle, Boston,
18 MA 02115, USA

19 ^e Institute of Innate Immunity, University Hospital Bonn, Sigmund-Freud-Str. 25, 53127 Bonn,
20 Germany

21 ^f German Center for Neurodegenerative Diseases (DZNE), Bonn, Germany.

22 ^g Department of General, Visceral and Transplant Surgery, University Hospital Tübingen, Hoppe-
23 Seyler-Str. 3, 72076 Tübingen, Germany

24 ^h Department of Clinical Pharmacology, University Hospital Tübingen, Auf der Morgenstelle 8, 72076
25 Tübingen, Germany

26 ⁱ iFIT – Cluster of Excellence (EXC 2180) "Image-Guided and Functionally Instructed Tumor Therapies",
27 University of Tübingen, Germany

28 ^j Institute of Organic Chemistry, University of Tübingen, Auf der Morgenstelle 18, 72076 Tübingen,
29 Germany

30 ^k Department of Pediatrics I, University Hospital Tübingen, Hoppe-Seyler-Str. 1, 72076 Tübingen,
31 Germany

32 ^l Interfaculty Institute of Microbiology and Infection Medicine, University of Tübingen, Elfriede-
33 Aulhorn-Str. 6, 72076 Tübingen, Germany

34 ^m Centre of Chronic Immunodeficiency, University Hospital Freiburg, Engesserstr. 4, 79108 Freiburg,
35 Germany

36 ⁿ Institute for Immunodeficiency, Center for Chronic Immunodeficiency (CCI), Medical Center, Faculty
37 of Medicine, Albert-Ludwigs-University of Freiburg, Germany

38 ^o DZIF – German Center for Infection Research, Satellite Center Freiburg, Germany

39 ^p CIBSS – Centre for Integrative Biological Signalling Studies, Albert-Ludwigs University, Freiburg,
40 Germany

41 ^q RESIST – Cluster of Excellence 2155 to Hanover Medical School, Satellite Center Freiburg, Germany

42 ^r Division of Infectious Diseases & Immunology, University of Massachusetts, 364 Plantation St,
43 Worcester, MA 01605, USA

44 **Contact information**

45 * to whom correspondence should be addressed: Alexander Weber; Interfaculty Institute for Cell
46 Biology, Department of Immunology, University of Tübingen, Auf der Morgenstelle 15, 72076

47 Tübingen, Germany; Tel. +49 7071 2987623; Fax. +49 7071 294759;
48 alexander.weber@uni.tuebingen.de

49 [§] Current address: CureVac AG, Paul-Ehrlich-Straße 15, 72076 Tübingen, Germany.

50 **Funding**

51 The study was supported by the Else-Kröner-Fresenius Stiftung (to ANRW), the Deutsche
52 Forschungsgemeinschaft (German Research Foundation, DFG) grants CRC TR156 “The skin as an
53 immune sensor and effector organ – Orchestrating local and systemic immunity” (to ZSB, FH and
54 ANRW) and We-4195/15-1 (to ANRW), University Hospital Tübingen (Fortüne Grant 2310-0-0 to XL
55 and ANRW), IFM Therapeutics (to ANRW), the “E-rare” program of the European Union, managed by
56 the DFG, grant code GR1617/14-1/iPAD (to BG), and the „Netzwerke Seltener Erkrankungen“ of the
57 German Ministry of Education and Research (BMBF, GAIN_ 01GM1910A, to BG) and the Damon
58 Runyon Cancer Research Foundation (to LA). Infrastructural funding was provided by the University
59 of Tübingen, the University Hospital Tübingen and the DFG Clusters of Excellence "iFIT – Image-
60 Guided and Functionally Instructed Tumor Therapies" (EXC 2180, to AW), “CMFI – Controlling
61 Microbes to Fight Infection (EXC 2124, to AW), “CIBSS – Centre for Integrative Signalling Studies”
62 (EXC 2189, to BG) and “RESIST – Resolving Infection Susceptibility” (EXC 2155, to BG). Gefördert
63 durch die Deutsche Forschungsgemeinschaft (DFG) im Rahmen der Exzellenzstrategie des Bundes
64 und der Länder - EXC 2180 (390900677), EXC 2124, EXC 2189 (390939984) and EXC 2155 (39087428).

65

66

67 **Abstract**

68 Inflammation is required for host defense as well as wound healing but wields enormous destructive
69 potential, highlighting the need for multiple ‘checks and balances’ [1]. The NLRP3 inflammasome, a
70 pivotal molecular machine for the maturation of IL-1 family pro-inflammatory cytokines [1], is
71 controlled by accessory proteins [2, 3], post-translational modifications [4, 5], localization [6, 7] and
72 oligomerization [8]. How these factors act in concert is unclear. We show that the established drug
73 target NLRP3 regulator, Bruton’s Tyrosine Kinase (BTK) [2, 9], integrates these levels of regulation to
74 boost inflammasome activity: by directly phosphorylating four conserved tyrosine residues in a
75 polybasic NLRP3 PYD-NACHT domain linker region, BTK weakens the interaction of NLRP3 with Golgi
76 phospholipids and localization. BTK activity also promotes NLRP3 oligomerization and subsequent
77 formation of inflammasomes. As NLRP3 tyrosine modification impacted on IL-1 β release, we propose
78 a novel BTK- and charge-mediated molecular phospho-switch to decisively regulate NLRP3 activity.
79 Collectively, our study highlights BTK as a ‘multi-layer regulator’ of the inflammasome and NLRP3
80 multi-tyrosine phosphorylation as a therapeutic target for restricting excess inflammation.

81 **Keywords**

82 NLRP3 inflammasome, Bruton’s Tyrosine Kinase (BTK), Interleukin-1, Inflammation, Ibrutinib,
83 Macrophage, X-linked agammaglobulinemia, Cryopyrin-associated periodic syndrome (CAPS).

84 **Introduction**

85 Inflammation mediated via the NLRP3 inflammasome supports the resolution of infections and
86 sterile insults but also contributes to pathology in multiple human diseases such as cryopyrin-
87 associated periodic fever syndromes (CAPS), gout, stroke or Alzheimer's disease, and atherosclerosis
88 [10, 11]. Thus, the NLRP3 inflammasome, a molecular machine maturing IL-1 family cytokines via the
89 activity of caspase-1, is tightly controlled on several levels: On the structural level, recent cryo-EM
90 studies demonstrated that the 3D conformation of NLRP3 is critical for NLRP3 oligomerization and
91 may depend on ADP/ATP binding [8]. In addition, NLRP3 binding proteins, such as NEK7, have been
92 shown to have an impact on inflammasome activity [3, 12]. Moreover, post-translational
93 modifications of NLRP3 enhance or reduce its activity by only partially elucidated mechanisms [5].
94 Finally, NLRP3 interacts dynamically with subcellular organelles such as the trans-Golgi network
95 (TGN): Whilst a polybasic region in the linker connecting the NLRP3 pyrin (PYD) and NACHT domains
96 appears to control NLRP3 phosphatidylinositol-4-phosphate (PtdIns4P) tethering at the disperse TGN
97 [6], dissociation from the TGN into the cytosol was proposed a requirement for the nucleation of
98 larger NLRP3 oligomers and, subsequently, the assembly of the complete inflammasome complexes,
99 including ASC and caspase-1 [7]. The cues instigating this shift in localization are not well understood.
100 Although multiple layers of NLRP3 regulation have been discovered, it is unclear how they are related
101 or even integrated on the cellular as well as on the molecular level. If individual regulators were to
102 provide this integration, they could be valuable targets to modulate inflammasome activity.

103 We and others have recently identified Bruton's tyrosine kinase (BTK) as a novel and therapeutically
104 relevant NLRP3 regulator [2, 13], which is rapidly activated upon NLRP3 inflammasome stimulation,
105 and interacts with NLRP3 and ASC in overexpression systems. Its genetic ablation led to reduced IL-
106 1 β secretion *in vitro* and, importantly, in human patients *ex vivo* [2]. BTK is a well-known cancer
107 target for which FDA-approved inhibitors such as ibrutinib exist (reviewed in Ref. [9]). Based on the
108 molecular mechanisms and chronic inflammatory processes observed in cancer diseases, targeting
109 NLRP3 via BTK also appears as an attractive therapeutic option in other diseases.

110 We report that BTK directly modifies NLRP3 at four tyrosine residues in the PYD-NACHT polybasic
111 linker, affecting NLRP3 PtdIns4P binding and Golgi enrichment. Consequently, ablation of BTK kinase
112 activity or tyrosine mutation decreased the formation of NLRP3 oligomers and IL-1 β release,
113 respectively. Our data suggest that this BTK-mediated phospho-tyrosine switch affects NLRP3 activity
114 via its 3D conformation and the charge of its polybasic linker affecting subcellular localization, and
115 emerges as an important control hub orchestrating NLRP3 inflammasome activation on multiple
116 levels.

117 **Results**

118 **BTK deficiency coincides with reduced NLRP3 tyrosine phosphorylation**

119 Based on previous work [2], we hypothesized that BTK and NLRP3 may engage in a direct kinase-
120 substrate relationship, whose elucidation might unravel novel molecular aspects of NLRP3
121 inflammasome regulation. We sought to test this in *Btk*-deficient primary murine BMDMs and in
122 PBMCs from patients with the genetic *BTK* deficiency, X-linked agammaglobulinemia (XLA). Evidently,
123 IL-1 β release upon nigericin stimulation was significantly reduced in BTK-deficient BMDMs and
124 patient-derived PBMC, respectively (Fig. 1A, B). Interestingly, in BMDMs, endogenous NLRP3
125 precipitated and interacted with endogenous BTK in WT but not *Btk* or *Nlrp3* KO BMDM (Fig. 1C),
126 irrespective of the BTK kinase inhibitor ibrutinib. Similarly, BTK co-immunoprecipitated with NLRP3 in
127 PBMCs from healthy donors (HDs) (Fig. 1D). Thus, in both human and murine primary immune cells
128 BTK and NLRP3 interact constitutively and independently of nigericin stimulation. This was also
129 confirmed by a cell-free *in vitro* pull-down involving only recombinant purified NLRP3 and BTK
130 proteins (Fig. 1E, Ref. [8] and Methods). We next tested whether BTK is able to phosphorylate NLRP3
131 upon nigericin treatment. In murine BMDMs (Fig. 1F) immunoprecipitated NLRP3 became rapidly
132 phospho-tyrosine (p-Y)-positive, in cells expressing *Btk* but not in *Btk* or *Nlrp3* KO cells. Similarly,
133 NLRP3 phosphorylation was also observed in healthy donor PBMCs (Fig. 1G), and lower in XLA PBMCs
134 (Fig. S1A). Importantly, treatment with λ -phosphatase abolished p-Y reactivity, further confirming the

135 phospho-antibody specificity. Thus, BTK and NLRP3 interact endogenously in primary immune cells
136 and BTK promotes NLRP3 tyrosine-phosphorylation upon nigericin stimulation.

137 **BTK kinase activity is required for NLRP3 tyrosine phosphorylation**

138 We next tested whether BTK kinase activity was required for NLRP3 tyrosine phosphorylation. Two
139 independent cell-free *in vitro* setups show that the presence of BTK was necessary and sufficient for
140 NLRP3 p-Y modification (Figs. 1H and S1B). However, in both PBMC and the *in vitro* setup NLRP3
141 tyrosine phosphorylation was blocked by ibrutinib treatment (Figs. 1I and S1B) and, thus, dependent
142 on BTK kinase activity. Next, HEK293T cells were transfected with NLRP3 and BTK, and treated with
143 or without BTK inhibitors. NLRP3 and BTK interacted independently of BTK kinase inhibitors ibrutinib
144 and acalabrutinib; however, NLRP3 tyrosine phosphorylation was abrogated in the presence of both
145 BTK kinase inhibitors (Fig. 1J), consistent with results in primary BMDM (*cf.* Fig. 1C). In contrast, the
146 NLRP3-specific inhibitor MCC950 [14] failed to prevent BTK-specific interaction and NLRP3 p-Y
147 positivity (Fig. 1J). Interestingly, the expression of kinase-dead (KD) BTK (K430E mutation, see Ref.
148 [9]) was not able to induce NLRP3 tyrosine phosphorylation, despite an intact interaction (Fig. 1K).
149 Similar results were obtained in the *in vitro* cell-free setup (*cf.* Fig. S1B). Thus BTK kinase activity
150 emerged as essential and sufficient for NLRP3 p-Y modification using primary immune cells, the
151 HEK293T system or purified recombinant proteins, indicative of a direct kinase-substrate
152 relationship.

153 **BTK phosphorylates four conserved tyrosine residues in the NLRP3 PYD-NACHT linker** 154 **domain**

155 To map the modified tyrosine residues in NLRP3, we compared Flag-tagged full-length with truncated
156 NLRP3 constructs [15] of only the PYD (1-93), the extended NACHT domain (94-534), which includes
157 an N-terminal linker domain (94-219) [8], and the LRR domain (535-1,036). BTK exclusively
158 phosphorylated the NLRP3 extended NACHT construct (Fig. 2B, C), ruling out Y816 [5] as the
159 phospho-site. Mutation of the nine tyrosines in the core NACHT domain (220-534, (Fig. 2D) to
160 phenylalanine (F) did not impact the level of phospho-NLRP3 detected upon BTK co-expression (Fig.

161 S3A, quantified in S3B). However, when the linker (94-219) tyrosines were targeted (Fig. 2E), mutated
162 Y168 showed partial but significant reduction of the p-Y signal, as shown by conventional
163 immunoblotting (Fig. 2F, quantified in G) and WES capillary electrophoresis analysis (Fig. 2H,
164 quantified in S3C), respectively. Thus, Y168 emerged as a novel putative phospho-tyrosine site in
165 NLRP3, specifically modified by BTK. Unfortunately, the linker region is not accessible to mass
166 spectrometric analysis (data from [16] plotted in Fig. S3D). Therefore, to assess the phosphorylation
167 of Y168 by alternative means, 15-mer peptides covering all linker tyrosines (*cf.* Fig 2E and Table S1)
168 were mixed with His-tagged BTK to assess peptide phosphorylation in a cell-free system. Following
169 BTK removal by anti-His beads, p-Y phosphorylation of the peptides was visualized by dot blot
170 analysis. While the majority of Y-containing peptides and all F-containing corresponding peptides
171 were not phosphorylated (Fig. S3E), the Y168-containing peptide showed strong tyrosine
172 modification (Fig. 2I). Of note, peptides containing Y136, Y140, or Y143 – either in combination or as
173 single tyrosines – were also phosphorylated (Fig. 2I), similar to peptides containing the sequences in
174 mouse NLRP3 (Y132, Y136, Y145 and Y164, see Fig. S3F). In HEK293T cells, combined mutations of
175 Y136, Y140, Y143 (“3Y>F”) and additionally Y168 to phenylalanine (“4Y>F”) consequently led to a
176 strong reduction of the p-Y signal, both in a FL-NLRP3 construct and when the linker was fused to an
177 mCitrine yellow fluorescent protein-HA sequence (here termed ‘hLinker-Cit-HA’, Fig. 2J). Consistent
178 with the only partial effect of Y168F mutation (*cf.* Fig. 2F-H), BTK is able to specifically modify not
179 only one, but rather four tyrosines – Y136, Y140, Y143 and Y168 – in the PYD-NACHT linker of human
180 (and murine) NLRP3 *in vitro*.

181 To gain a structural insight, we mapped the sites in a recent cryo-EM structure of an NLRP3-NEK7
182 complex (Ref. [8], Fig. 2K and S4A). Interestingly, Y136, Y140 and Y143 were found in a helical region
183 proposed to contact the PYD for ASC recruitment [8]. Further, Y168, which maps to the vicinity of
184 several likely pathogenic CAPS mutations (*cf.* Fig. S2), was adjacent to a putative ADP molecule and
185 might thus influence nucleotide binding (Fig. 2L, M). Interestingly, all identified, and BTK-modified, Y
186 residues were strongly conserved in other NLRP3 sequences, further highlighting their potential

187 functional relevance (Fig. S4B). Collectively, our results indicate that BTK directly modifies multiple
188 highly conserved tyrosines within a functionally important domain in NLRP3 that could impact
189 downstream steps in the assembly of the oligomeric inflammasome complexes.

190 **BTK-mediated phosphorylation sites affect PI4P binding**

191 Chen and Chen recently identified a ‘polybasic’ motif (K127-130 in mouse; K127 and K129-130 in
192 human NLRP3) as critical for NLRP3 charge-dependent binding to Golgi phosphatidylinositol
193 phosphates (PtdInsPs) and inflammasome nucleation [6]. Unexpectedly, Y136, Y140 and Y143
194 precisely mapped to this polybasic motif in the NLRP3 PYD-NACHT linker, and interdigitate with the
195 basic residues mediating the proposed NLRP3 interaction with negatively charged membrane
196 phospholipids (Fig. 3A). Given that the mutation of three positively charged residues (K127, K129,
197 K130) in the mNLRP3 polybasic region to alanine (K>A) is sufficient to abrogate PtdInsP binding [6],
198 we hypothesized that by BTK phosphorylation of Y136, Y140 and Y143 the proposed charge
199 attraction of NLRP3 might weaken NLRP3-Golgi interactions. [6, 7]. Charge computations suggested
200 that at cytoplasmic pH 7.4, the net charge of the unphosphorylated linker sequence (+7.28) shifts to
201 +2.01 for a 3x human NLRP3 Y-phosphorylated sequence (Fig. 3B), and from +8.33 to +3.06 for mouse
202 NLRP3. Indeed clear differences between synthetic phospho- and non-phospho versions of the
203 Y136/Y140/Y143-containing peptides from both human and mouse NLRP3 were discernible in pH
204 titrations (Fig. S5A). Furthermore, in the NLRP3-NEK7 structure the 3x phospho-modification is
205 calculated to cause a significant change in the computed surface charge of a ‘hypothetically active’
206 NLRP3 state [8] towards negative values (Fig. S5B). We therefore hypothesized tyrosine
207 phosphorylation by BTK might weaken interactions with the negatively charged PtdIns4Ps (PI4Ps).
208 Consistently, the binding of 4xY>E, i.e. phospho-mimetic, mutant human NLRP3 linker-Cit-HA fusion
209 protein to PI4P beads [6] was reduced compared to the corresponding WT construct (Fig. 3C). This
210 was further confirmed by the fusion of the murine NLRP3 polybasic region to GFP-Flag (mPBR-GFP-
211 Flag, construct as in Ref. [6]): Despite equal expression, the Y>E construct bound PI4P beads less
212 strongly than WT (Fig. 3D). Reduced binding was also observed for the corresponding K>A mutant,

213 which is known to be defective in PI4P binding based on charge alteration [6]. To test whether BTK
214 activity might consequently affect Golgi localization, we fractionated different stimulated BMDM
215 lysates into S100 (soluble, cytosol), P5 (heavy membrane, Golgi and mitochondria) and P100 (light
216 membrane, ER and polysomes) fractions and probed them for NLRP3. BTK, whose PH domain also
217 binds PtdInsPs (references in [17], was also analyzed and found to localize similarly to NLRP3 (Fig. 3E,
218 Fig. S5C), in keeping with earlier interaction analyses (*cf.* Fig. 1C, F). As expected [6], in both WT and
219 *Btk* KO BMDMs, NLRP3 was detectable in the P5 fraction upon LPS treatment, indicating that BTK is
220 not essential for initial NLRP3 localization *towards* P5 membranes (Fig. 3E, Fig. S5C). However,
221 nigericin stimulation in WT BMDM coincided with progressive depletion of NLRP3 from the P5
222 fraction within 20 min, consistent with the timing of phosphorylation in these cells (*cf.* Fig 1F).
223 Conversely, *Btk* KO BMDMs did not show dissociation within this time, indicating NLRP3 interaction
224 with Golgi membranes remain more stable in the absence of BTK, which is likely attributable to
225 charge-mediated PtdInsP-interactions [6]. Collectively, these experiments show that both, the BTK-
226 modified tyrosine residues in the NLRP3 linker and the presence of BTK, have an impact on NLRP3
227 linker-PI4P binding and subcellular fractionation of NLRP3; most probably via affecting linker charge
228 (*cf.* Fig. 3A, B and S5B).

229 **BTK kinase activity affects NLRP3 oligomerization and IL-1 β release**

230 A recent study proposed that NLRP3 release from the Golgi was required for ASC engagement and
231 full inflammasome assembly [7]. We therefore explored whether BTK kinase activity affected
232 subsequent full inflammasome assembly, e.g. by recruiting ASC into complex formation. Indeed,
233 native PAGE of nigericin-stimulated WT and *Btk* KO BMDM lysates (Fig. 4A) or BTK inhibitor- vs
234 vehicle-treated *Pycard* (ASC) KO (Fig. 4B) showed reduced NLRP3 oligomers in BTK-deficient or –
235 inhibited samples, and lower ASC cross-linking (Fig. 4C). Size exclusion chromatography of untreated
236 WT cell lysates showed that BTK and NLRP3 co-eluted in the high MW fraction (>1,100 KDa).
237 Consistent with native PAGE in *Btk* KO or WT lysates from ibrutinib-treated cells, elution shifted to
238 lower molecular weight complexes (Fig. 4D, E). Ablation of BTK activity, thus, appeared to

239 compromise the subsequent ability of NLRP3 to oligomerize into large MW cytosolic inflammasomes
240 and to assemble with ASC. To show that BTK-modified tyrosine residues - and the effects of BTK
241 described so far - also had an impact on IL-1 β release, NLRP3-deficient immortalized macrophages
242 were retrovirally transduced with WT or tyrosine-mutated (4xY>F) NLRP3-T2A-mCherry constructs,
243 allowing for cell sorting for equal protein expression (Fig. 4F). Compared to WT-transduced cells, cells
244 with the 4xY>F construct failed to restore nigericin- and R837 (imiquimod)-dependent IL-1 β release
245 (Fig. 4G). Conversely, TNF release, which is NLRP3- and BTK- independent [2], was comparable
246 between cell lines (Fig. 4H). Likewise, IL-1 β release upon stimulation with the NLRP3- and BTK-
247 independent [2] AIM2 inflammasome stimulus, poly(dA:dT), was comparable between WT and
248 mutant cells (Fig. 4G,H). The data show that the BTK-modified tyrosines identified here play an
249 important role for full NLRP3 inflammasome activity and subsequent IL-1 β release.

250 **Discussion**

251 The mechanism of action for NLRP3 inflammasome activation has been intensely studied for years
252 and recent work has uncovered that NLRP3 interaction with [6] and dissociation from [7] the Golgi
253 may be critical events. Using both biochemical and cellular assays involving human and murine
254 primary cells, we identify BTK to directly participate in these processes at the level of NLRP3,
255 providing a molecular rationale: direct phosphorylation of four conserved and functionally important
256 tyrosine residues in the NLRP3 polybasic linker motif weakened NLRP3 PtdIns4P interactions, which
257 was most probably based on neutralizing the net surface charge. As a result, NLRP3 retention to the
258 Golgi is seemingly shorter, with the consequence of enhanced NLRP3 inflammasome oligomerization,
259 ASC association, and increased IL-1 β secretion. Our data suggest that BTK-mediated phosphorylation
260 of multiple NLRP3 tyrosines serves as a molecular switch of NLRP3 inflammasome activity.
261 Modification, localization, and oligomerization of NLRP3 have been recognized to be important but,
262 supposedly hierarchically separate layers of NLRP3 inflammasome regulation and, thus,
263 inflammation; our data indicate that these layers can be integrated and interconnected by BTK: By
264 interpreting the most basal determinant such as protein sequence, BTK appears to integrate post-
265 translational modification, surface charge, interaction with organelles, and ultimately assembly of a
266 highly oligomeric molecular machinery (Fig. S6). Such a dense and interconnected network of
267 regulation would be in line with the critical needs to tightly control excessive IL-1 β release to prevent
268 pathologies. Our data indicate that BTK seems to license IL-1 β levels via the regulatory events
269 characterized here, and implicates that NLRP3 phosphorylation might serve as a biomarker and
270 therapeutic target for early NLRP3 activation. Collectively, our work provides both a rationale as well
271 as concrete targeting strategies that may be applied to block excess IL-1 β production in acute
272 inflammasome-related diseases.

273 **Abbreviations**

274 AIM2 – Interferon-inducible protein absent in melanoma 2; ASC – Apoptosis-associated speck-like
275 protein containing a Caspase activation and recruitment domain (CARD); BMDM – bone marrow-
276 derived macrophages; BTK – Bruton’s Tyrosine Kinase; FDA – Food and Drug Administration; CAPS –
277 Cryopyrin-associated periodic syndrome; GM-CSF - Granulocyte-macrophage colony-stimulating
278 factor; HD – healthy (blood) donor; HEK – human embryonic kidney; IFN – Interferon; IL –
279 Interleukin; KD – kinase-dead; LPS – Lipopolysaccharide; LRR – leucine-rich repeat; NEK7 – NIMA
280 related kinase 7; NACHT – NAIP, CIITA, HET-E and TEP1; NLR – Nod-like receptor; NLRP3 – NACHT,
281 LRR and PYD domains-containing protein 3; PBMC - peripheral blood mononuclear cell; PH –
282 Pleckstrin homology; PtdIns4P – phosphatidylinositol-4-phosphate; PMA - Phorbol-12-myristate-13-
283 acetate; p-Y – phospho-tyrosine; PYD – Pyrin domain; SH - Src homology; TGN – trans-Golgi network;
284 TH - Tec homology; TLR – Toll-like receptor; TNF – Tumor necrosis factor; XLA - X-linked
285 agammaglobulinemia.

286 **Materials and Methods**

287 **Reagents.** Nigericin and Lipopolysaccharide (LPS) were purchased from Invivogen, ATP from Sigma,
288 ibrutinib and acalabrutinib from Selleckchem, recombinant Granulocyte-macrophage colony-
289 stimulating factor (GM-CSF) from Prepro-Tech, Ficoll from Merck Millipore. Peptides (EMC
290 Microcollections Tübingen or synthesized in house) and antibodies are listed in Tables S1 and S2,
291 respectively.

292 **Peptides.** Synthetic peptides were produced by standard 9-fluorenylmethyloxycarbonyl/tert-butyl
293 strategy using peptide synthesizers P11 (Activotec, Cambridge, UK) or Liberty Blue (CEM, Kamp-
294 Lintfort, Germany). Purity was assessed by reversed phase HPLC (e2695, Waters, Eschborn, Germany)
295 and identity affirmed by nano-UHPLC (UltiMate 3000 RSLCnano) coupled online to a hybrid mass
296 spectrometer (LTQ Orbitrap XL, both Thermo Fisher, Waltham, MA, USA). Lyophilized peptides were
297 purified by standard HPLC. For certain peptides a pH titration with NaOH was performed using

298 standard procedures. For *in vitro* assays peptides were dissolved at 10 mg/ml in dimethyl sulfoxide
299 (DMSO) and diluted 1:10 in bidistilled H₂O. Frozen aliquots were further diluted in cell culture
300 medium and sterile filtered if necessary.

301 **Plasmid constructs.** ASC, NLRP3 and BTK coding sequences in pENTR clones were generated as
302 described in [18]. Truncated Flag-tagged NLRP3 constructs were a kind gift of F. Martinon, Lausanne,
303 Switzerland [15]. Constructs for the human PYD-NACHT linker (residues 94-219) fused to mCitrine-HA
304 or the murine polybasic motif (residues 127-146) fused to GFP-Flag (as in [6]) were synthesized by
305 GeneWiz. Point mutations in BTK and NLRP3 were subsequently introduced using QuikChange II Site-
306 Directed Mutagenesis Kit from Agilent Technologies, following the manufacturer's instructions.
307 Presence of the desired mutation and absence of unwanted regions in the entire CDS was confirmed
308 by automated DNA sequencing.

309 **Study subjects and blood sample acquisition.** CAPS patients were recruited at the Department of
310 Pediatrics, University Hospital Tübingen and XLA patients at the Centre of Chronic Immunodeficiency,
311 University Hospital Freiburg, healthy blood donors at the Interfaculty Institute of Cell Biology,
312 Department of Immunology, University of Tübingen. All patients and healthy blood donors included
313 in this study provided their written informed consent before study participation. Approval for use of
314 their biomaterials was obtained by the respective local ethics committees, in accordance with the
315 principles laid down in the Declaration of Helsinki as well as applicable laws and regulations. XLA
316 patients were clinically identified and genetically characterized as described in [2].

317 **Mice.** *Btk* KO [19] and *NLRP3* KO (Jackson stock No: 021302) and wild type C57BL/6J (Jackson)
318 colonies were maintained in specific-pathogen free conditions under regular hygiene monitoring. All
319 animal experiments were approved by local authorities and performed in accordance with local
320 institutional guidelines and animal protection laws, including specific locally approved protocols for
321 sacrificing.

322 **Cell culture.** All cells were cultured at 37 °C and 5% CO₂ in DMEM or RPMI supplemented with 10%
323 fetal calf serum, L-glutamine (2 mM), penicillin (100 U/ml), streptomycin (100 µg/ml) (all from
324 Thermo Fisher).

325 **Isolation and stimulation of primary human immune cells.** Peripheral blood mononuclear cells
326 (PBMCs) from healthy donors and patients were isolated from whole blood using Ficoll density
327 gradient purification, primed with 10 ng/ml LPS for 3 h, and in some cases treated with 60 µM
328 ibrutinib before stimulation with 15 µM nigericin for the indicated periods of time.

329 **Isolation of primary bone marrow-derived macrophages (BMDMs).** Bone marrow (BM) cells were
330 isolated from femurs and tibiae of 8-12 week old mice, grown and differentiated using GM-CSF (M1
331 polarization) as described [2].

332 **Expression and purification of recombinant BTK, NEK7 and NLRP3.** The plasmids encoding NLRP3
333 with the deleted pyrin domain (amino acids 134–1034) for MBP-fusion protein expression in Bac-to-
334 Bac system (Thermo Fisher) and human NEK7 for His-SUMO fusion protein expression in *E. coli* BL21
335 (DE3) were described recently [8]. For NLRP3 expression the baculovirus of NLRP3 was prepared
336 using the Bac-to-Bac system (Thermo Fisher). Protein expression was induced by infection of Sf9 cells
337 with 1% v/v of baculovirus. 48 h after infection cells were lysed by sonication in buffer containing 30
338 mM HEPES, 200 mM NaCl, 2 mM 2-mercaptoethanol and 10% glycerol at pH 7.5 with freshly added
339 protease inhibitor cocktail (Sigma). The supernatant was incubated with 3 ml amylose resin at 4°C for
340 1 h and subjected to gravity flow. NLRP3 protein was eluted with 50 mM maltose and further purified
341 with size-exclusion chromatography on Superose 6 10/300 GL column (GE Healthcare) equilibrated
342 with buffer containing 30 mM HEPES, 150 mM NaCl and 2 mM β-mercaptoethanol at pH 7.5. NEK7
343 was overexpressed in *E. coli* BL21 (DE3) overnight at 18 °C after induction with 0.1 mM isopropyl-β-d-
344 thio-galacto-pyranoside after optical density at 600 nm reached 0.8. Cells were lysed by sonication in
345 buffer containing 50 mM HEPES, 500 mM NaCl, 5 mM MgCl₂, 10 mM imidazole, 10% glycerol and 2
346 mM β-mercaptoethanol at pH 7.5 with freshly added protease inhibitor cocktail (Sigma). The His-
347 SUMO-fusion NEK7 was purified by affinity chromatography using Ni-NTA beads (Qiagen) followed by

348 size-exclusion chromatography on Superdex 200 10/300 GL column (GE Healthcare) equilibrated with
349 buffer containing 30 mM HEPES, 150 mM NaCl and 2 mM β -mercaptoethanol at pH 7.5. WT and
350 kinase-dead mutant BTK were overexpressed in Expi293 cells (Thermo Fisher) using transient
351 transfection with poly-ethylenimine 25K (Polysciences). Cells were harvested 96 h post transfection
352 and lysed in buffer containing 50 mM HEPES, 150 mM NaCl, 2 mM 2-mercaptoethanol and 10%
353 glycerol at pH 7.5 with freshly added protease inhibitor cocktail (Sigma). The FLAG-fusion proteins
354 were subjected to affinity chromatography using anti-FLAG M2 affinity gel (Millipore Sigma), eluted
355 with 3xFLAG-peptide (Millipore Sigma) and further purified by size-exclusion chromatography on
356 Superdex 200 10/300 GL column (GE Healthcare) equilibrated with buffer containing 30 mM HEPES,
357 150 mM NaCl and 2 mM β -mercaptoethanol at pH 7.5. Proteins were concentrated to 2-7mg/ml,
358 flash-frozen in liquid nitrogen and stored at -80 °C.

359 **In vitro pull-downs.** MBP-tagged NLRP3 (2 μ M) was mixed with 4 μ M His-SUMO-NEK7 or wild type or
360 mutant FLAG-BTK in buffer containing 30 mM HEPES, 150 mM NaCl and 2 mM β -mercaptoethanol at
361 pH 7.5, and incubated for 30 min at 30°C. The mixture was further incubated for 1 h with 40 μ l
362 amylose resin and washed twice with 500 μ l of the same buffer, followed by 1 h elution with 50 mM
363 maltose. 30% and 70% of the sample was loaded as input and elution fractions, respectively, and
364 analyzed by SDS-PAGE and immunoblot using monoclonal Anti-Flag® M2-Peroxidase (HRP) or anti-p-
365 Y antibody (Sigma-Aldrich).

366 **ELISA.** Human and murine IL-1 β , IL-6 or TNF in supernatants were determined by ELISA using half-
367 area plates using kits by R&D Systems and Biolegend, determining triplicate points on a standard
368 plate reader.

369 **Co-immunoprecipitation and immunoblot.** PBMCs or BMDMs were primed with LPS and stimulated
370 with nigericin, washed with cold PBS and immediately lysed in RIPA lysis buffer containing
371 protease/phosphatase inhibitors (Roche). A sample of the cleared lysate was taken before addition of
372 the primary antibody (see Table S2). After 18 hours of rotation in the cold room, magnetic bead
373 coupled secondary antibody (Protein G Dynabeads, Thermo Fisher) was added for another 90 min.

374 The beads were then washed three times with lysis buffer, resuspended in SDS loading buffer and
375 boiled. HEK293T were transfected using CaPO₄ and lysed 48 hours later in RIPA buffer with
376 protease/phosphatase inhibitors (Roche). Cleared lysates were subjected to immunoprecipitation of
377 the NLRP3-HA or NACHT-FLAG fusion protein with Dynabeads (Sigma-Aldrich), or with agarose beads
378 covered with PI4P (P-B004a, Echelon Biosciences). Washed beads were boiled in loading buffer and
379 applied to standard SDS-PAGE on Thermo Fisher pre-cast gels, followed by immunoblot according to
380 the antibody manufacturer's instructions. Membranes were exposed using Peqlab Fusion FL camera
381 and FusionCapt Advance software. Quantification was conducted using the same software.

382 **WES capillary electrophoresis.** 3 µl of the prepared Western Blot lysates were run on ProteinSimple
383 WES instrument according to the manufacturer's instructions. Data were analyzed with the Compass
384 for SW software comparing the p-NLRP3 signal with the heavy chain signal from the same run as an
385 internal control.

386 **Native PAGE.** BMDMs were stimulated and lysed in RIPA lysis buffer without SDS: Lysates were
387 centrifuged at 2,300 x *g* for 10 min to pellet DNA. Supernatant was centrifuged at 16,100 x *g* for 25
388 min and the pellet was resuspended in Native PAGE sample buffer (Thermo Fisher). The samples
389 were loaded onto NuPage 3-8% Tris-Acetate gels (Thermo Fisher) without boiling and native PAGE
390 was conducted using Tris-Glycine running buffer (Thermo Fisher). The gel was soaked in 10% SDS
391 solution for 10 min before performing semi-dry transfer and continuing with conventional
392 immunoblot.

393 **Crosslinking of ASC oligomers.** BMDMs were primed with LPS and treated with ibrutinib and
394 nigericin. Cells were lysed in RIPA lysis buffer and pellets were cross-linked using DSS and analyzed as
395 described in [20].

396 **Size exclusion chromatography.** BMDMs were stimulated and lysed in 50 mM Tris-HCl pH 7.4, 1%
397 NP-40, and 150 mM NaCl. 100 µl cleared lysate were loaded on a Superdex 200 Increase 10/300 GL
398 (GE Healthcare) column and proteins were eluted using ÄKTA Purifier (GE Healthcare) and buffer 50

399 mM Tris-HCL pH 7.4 and 150 mM NaCl with 0.25 ml/min flow. 200 μ l fractions were collected and
400 analyzed via Western-Blot.

401 **In vitro kinase assay.** For results in Fig. 1H, recombinant NLRP3 from Novus Biologicals (H00114548-
402 P01) and BTK from Sino Biological (10578-H08B) or Abcam (ab205800) were incubated at 30 °C for 3
403 hours using CST kinase buffer (#9802) in the presence of 2 mM ATP. As a negative control,
404 recombinant Posi-Tag Epitope Tag Protein (Biolegend) was used. Before and after kinase assay
405 samples were boiled and analyzed via SDS PAGE and Western Blot. For results in Fig. S1B, NLRP3 and
406 BTK (WT or KD) were purified as described above. For reaction 2 μ M MBP-tagged NLRP3 was mixed
407 with or without 0.2 μ M purified FLAG-tagged BTK in buffer containing 30 mM HEPES, 150 mM NaCl,
408 12.5 mM MgCl₂, 2.5 mM ATP and 2 mM β -mercaptoethanol at pH 7.5 in presence or absence of
409 ibrutinib (Selleckchem, cat. S2680). The mixture was incubated at 30°C and equal aliquots were taken
410 at indicated time points. Samples were analyzed by SDS-PAGE and immunoblot using anti-p-Y
411 antibody (Cell signaling, cat. 8954S).

412 **Dot blot analysis.** Synthetized peptides were incubated with recombinant BTK (Sino Biologicals) for 3
413 h in CST kinase buffer (#9802) supplemented with 2 mM ATP. Next, the samples were boiled and
414 anti-His magnetic beads (Dynabeads™ His-Tag Isolation and Pulldown, Thermo Fisher) were added to
415 deplete the samples of phosphorylated BTK. The samples were cleared from the magnetic beads and
416 the supernatants were manually spotted on a nitrocellulose membrane. The dried spots were stained
417 using the Pierce reversible protein stain to visualize total peptide amounts. Then the membrane was
418 blocked with 5% BSA in TBS-T and conventional anti-phospho-Tyrosine primary and secondary
419 antibody incubation steps followed.

420 **Subcellular fractionation.** Cells were homogenized using a 10 ml syringe and 27 G x 19 mm needles
421 in homogenization buffer (0.25 M sucrose, 10 mM Tris HCl (pH 7.5), 10 mM KCl, 1.5 mM MgCl₂,
422 protease inhibitor (Roche) and PhosStop (Roche)). Homogenized cells were centrifuged at 1,000 x *g*
423 for 5 min to remove the nucleus. The supernatant was centrifuged at 5,000 x *g* for 10 min to obtain a

424 heavy membrane fraction (pellet, P5). The supernatant was centrifuged 100,000 x *g* for 20 min to
425 separate a light membrane fraction (S100) from the cytosol. P5 and S100 were washed once with
426 homogenization buffer and then used for sucrose gradient ultracentrifugation, separately. For
427 sucrose gradient ultracentrifugation, a continuous 15-45% (w/w) sucrose gradient was prepared in
428 10 mM Tris-HCl (pH 7.5), 20 mM KCl, and 3 mM MgCl₂) using a Biocomp Gradient Station (Biocomp
429 Instruments, Fredrickton, NB, Canada). P5 or S100 was loaded on top of the gradient and centrifuged
430 at 170,000 x *g* for 3 h. The gradient was fractionated into 12 fractions of 1.1 ml using the fraction
431 collector module of a Biocomp Gradient Station.

432 **Ptd4InsP bead binding assays.** HEK293T cells were transfected with HA-tagged human WT or Y>E
433 PYD/NACHT linker (residues 94-219)-mCitrine-HA constructs. Cells were lysed in RIPA buffer and PI4P
434 (Echelon Biosciences, P-B004A) or the same amount of control beads (Echelon Biosciences, P-B000)
435 were added to cleared lysates and incubated for 1.5 h on 4 °C while rotating. Beads were then
436 washed 3 times with RIPA buffer, boiled and bound proteins were analyzed via immunoblot.
437 Alternatively, cells were transfected with WT, Y>E or K>A Flag-tagged murine polybasic region
438 (residues 127-146)-GFP-Flag constructs, adopted from [6]. PI4P beads or control beads were blocked
439 beforehand in 2% BSA, 0.5% NP-40 and 200 µg/ml Flag peptide (Sigma-Aldrich, F3290) for 2 h at 4°C.
440 Transfected cells were then lysed in RIPA buffer and the expressed proteins were purified using Anti-
441 FLAG® M2 Magnetic Beads (M8823, Merck). Beads were washed 3x with RIPA buffer and boiled to
442 elute the purified polybasic region. Blocked PI4P beads or the same amount of control beads were
443 added to the eluted protein, and incubated for 1.5 h on 4°C while rotating. Beads were then washed
444 3x8 min with RIPA buffer, resuspended in LDS sample buffer, boiled, and bound protein was analyzed
445 using immunoblot.

446 **Reconstitution and analysis of NLRP3-deficient immortalized macrophages.** NLRP3-deficient
447 immortalized macrophages [21] were retrovirally transduced with NLRP3 (WT or 4xY>F)-Flag-T2A-
448 mCherry constructs as described in [21] and subsequently sorted for similar expression of mCherry.
449 Similar NLRP3 expression was confirmed by anti-Flag immunoblot of cell lysates. Cells were seeded at

450 1×10^5 cells/well in a 96 well plate in 100ul, primed with LPS (200 ng/ml) for 3h and inflammasome
451 stimuli in optiMEM added as follows: nigericin at 8 μ M for 1.5 h, R837 (imiquimod) at 20 ng/ml for 2h
452 or poly(dA:dT) at 200 ng per well with 0.5 μ l lipofectamine 2000 for 4 h. IL-1 β and TNF were
453 subsequently determined by IL-1 β and TNF HTRF assay respectively (Cisbio; 62MIL1BPEH and
454 62MTNFAPEG).

455 **NLRP3 sequence analysis, structure inspection and charge prediction.** NLR sequences were
456 retrieved from UniProt and ClustalW aligned within Geneious R6 software. A hypothetical active
457 conformation of NLRP3 was modeled based on NLRP3-NEK7 structure in an inactive state (PDB 6NPY)
458 [8]. NACHT domain reorganization and hypothetical NLRP3 oligomerization was generated, based on
459 the NLRC4 oligomer (PDB 3JBL) as a homology model template by introduction of a 90° rotation of
460 NBD-HD1 module [8]. Phosphorylation of tyrosine residues of interest was performed in Pymol
461 (Schrödinger) using the PyTMs plugin [22]. Electrostatic potential of the solvent accessible surface of
462 phosphorylated and non-phosphorylated NLRP3 models was calculated with PBEQ-Solver online
463 visualization tool (<http://www.charmm-gui.org> [23-25] and visualized with Pymol. Protein net
464 charges of the Y136, Y140 and Y143-containing linker were conducted with ProtPi (www.protpi.ch).

465 **Statistics.** Experimental data was analyzed using Excel 2010 (Microsoft) and/or GraphPad Prism 6, 7
466 or 8, microscopy data with ImageJ/Fiji, flow cytometry data with FlowJo 10. Normal distribution in
467 each group was always tested using the Shapiro-Wilk test first for the subsequent choice of a
468 parametric (ANOVA, Student's *t*-test) or non-parametric (e.g. Friedman, Mann-Whitney U or
469 Wilcoxon) test. *p*-values ($\alpha=0.05$) were then calculated and multiple testing was corrected for in
470 Prism, as indicated in the figure legends. Values <0.05 were generally considered as statistically
471 significant and denoted by * throughout. Comparisons were made to unstimulated control, unless
472 indicated otherwise, denoted by brackets.

473 **Figure Captions**

474 **Figure 1: NLRP3 directly interacts and is tyrosine phosphorylated by BTK.** (A, B) IL-1 β release
475 (triplicate ELISA) from WT vs *Btk* KO BMDM (A, n=5 each) or XLA vs healthy donor (HD) PBMCs (B,
476 n=3-6). (C, D) Co-IP of NLRP3 from WT, *Btk* KO or *Nlrp3* KO BMDM (n=3) or ibrutinib-treated PBMC
477 lysates (n=2). (E) *In vitro* pulldown of FLAG-tagged BTK or His-SUMO-tagged NEK7 by MBP-tagged
478 NLRP3 (n=3). (F, G) as in C and D, respectively, but with anti-phospho-tyrosine (p-Y) IP (n=3 or 5,
479 respectively). (H) as in E but using two different commercial suppliers, A and B, of recombinant BTK.
480 PosiTag = specificity control. (I) as in G but with ibrutinib pre-treatment (n=2). (J, K) IPs from HEK293T
481 cells transfected with NLRP3 and BTK WT or kinase dead (KD) constructs, or treated with inhibitors
482 (n=2 each). A and B represent combined data (mean+SD) from 'n' biological replicates (each dot
483 represents one mouse or patient/HD). C-K are representative of 'n' biological (HD or mouse) or
484 technical replicates. * p<0.05 using Student's *t*-test (A) or one-way ANOVA with Dunnett's correction
485 (B).

486 **Figure 2: BTK phosphorylates the PYD-NACHT linker.** (A) NLRP3 domains (UniProt ID Q96P20). (B) IP
487 from HEK293T cells transfected with NLRP3 and BTK constructs (n=3). (C) as in B but including
488 ibrutinib (n=3). (D) Positions of targeted tyrosine residues. (E) Linker region including polybasic motif.
489 (F) as in B but using Y to F point mutants and WT or kinase-dead (KD) BTK plasmids (n=4). (G)
490 Quantification of F. (H) WES capillary electrophoresis of IP p-NLRP3 (n=3). (I) Dot blot of BTK kinase
491 assay with 15-mer synthetic peptides (n=3). (J) as in F but also NLRP3 linker (WT or Y-mutated) fused
492 to mCitrine-HA (n=3). (K) Tyrosines (red) highlighted in model of NLRP3 (blue)-NEK7 (yellow) complex
493 (pdb: 6NPY). Close up view on dimer interface (L) and putative nucleotide binding site (M). G
494 represents combined data (mean+SD) from 'n' biological replicates (each dot represents one
495 replicate). B, C, F, H-J are representative of 'n' technical replicates. * p<0.05 according to one sample
496 *t*-test (G).

497 **Figure 3: BTK phosphorylation of the NLRP3 polybasic motif enables Golgi/PtdIns4P dissociation.**
498 (A, B) Charge distribution (A) and ProtPi charge computation (B) of unmodified (3xY) and phospho-

499 peptide polybasic motif. (C) NLRP3 linker-Cit-HA constructs precipitated with PI4P beads (n=2). (D) as
500 in C but murine NLRP3 polybasic region fused to GFP-HA (mPBR-GFP-HA, n=3). (E) Subcellular
501 fractionation of nigericin-treated WT or *Btk* KO BMDM lysates (n=2). In C-E one representative
502 example of 'n' technical replicates is shown.

503 **Figure 4: BTK modification affects NLRP3 oligomerization and IL-1 β release.** (A-C) WT, *Btk* KO, *Nlrp3*
504 KO or *Pycard* (ASC) KO BMDM stimulated and respective lysates analyzed directly by native PAGE (A,
505 n=2 and B, n=4) or ASC cross-linked in the pellet (C, n=4) and/or analyzed by SDS-PAGE. (D) as in A
506 but size exclusion chromatography (SEC) fractions (n=3). (E) as in D comparing inhibitor treated WT
507 BMDM or *Btk* KO BMDM lysates (n=3). (F-H) NLRP3 expression levels (F), IL-1 β (G) or TNF (H) release
508 from WT or 4xY>F NLRP3-reconstituted NLRP3-deficient iMacs (n=3). G-H represent combined data
509 (mean+SD) from 'n' technical replicates. A-F are representative of 'n' biological (mice) or technical
510 replicates. * p<0.05 according to one-way ANOVA (H) or ANOVA with Sidak correction (G).

511 **Author contributions**

512 ZAB, XL, SD, HK, KB, LA, AM, MM, PD, ML, FH, SS, ATA, OOW, NAS, SW and ANRW performed
513 experiments; ZAB, XL, SD, HK, LA, SS, ML, MM, PD, FH, NAS, SW and ANRW analyzed data; MWL, JKD,
514 AD and BG were involved in patient recruitment and sample acquisition; ZAB and ANRW wrote the
515 manuscript and LA, PD, MWL, SS, ATA, SW, HW and EL provided valuable comments. All authors
516 approved the final manuscript. ANRW and ZAB conceived and coordinated the study. *S.D.G.*

517 **Acknowledgements**

518 We gratefully acknowledge Philipp Oesterhelt, Frank Essmann and Sven Hülsmann for assistance with
519 confocal microscopy, Ulrich Wulle for help with peptide synthesis and Yamel Cardona Gloria for
520 helpful comments. We thank Xiaowu Zhang and Felix Meissner for helpful advice on kinase target
521 residue identification and mass spectrometry, respectively. We thank all study subjects and their
522 families for participating in the study.

523 **References**

- 524 1. Mangan, M.S.J., et al., *Targeting the NLRP3 inflammasome in inflammatory diseases*. Nat Rev
525 Drug Discov, 2018. **17**(8): p. 588-606.
- 526 2. Liu, X., et al., *Human NACHT, LRR, and PYD domain-containing protein 3 (NLRP3)*
527 *inflammasome activity is regulated by and potentially targetable through Bruton tyrosine*
528 *kinase*. J Allergy Clin Immunol, 2017.
- 529 3. He, Y., et al., *NEK7 is an essential mediator of NLRP3 activation downstream of potassium*
530 *efflux*. Nature, 2016. **530**(7590): p. 354-7.
- 531 4. Py, B.F., et al., *Deubiquitination of NLRP3 by BRCC3 critically regulates inflammasome*
532 *activity*. Mol Cell, 2013. **49**(2): p. 331-8.
- 533 5. Song, N. and T. Li, *Regulation of NLRP3 Inflammasome by Phosphorylation*. Front Immunol,
534 2018. **9**: p. 2305.
- 535 6. Chen, J. and Z.J. Chen, *PtdIns4P on dispersed trans-Golgi network mediates NLRP3*
536 *inflammasome activation*. Nature, 2018. **564**(7734): p. 71-76.
- 537 7. Zhang, Z., et al., *Protein kinase D at the Golgi controls NLRP3 inflammasome activation*. J Exp
538 Med, 2017. **214**(9): p. 2671-2693.
- 539 8. Sharif, H., et al., *Structural mechanism for NEK7-licensed activation of NLRP3 inflammasome*.
540 Nature, 2019. **570**(7761): p. 338-343.
- 541 9. Weber, A.N.R., et al., *Bruton's Tyrosine Kinase: An Emerging Key Player in Innate Immunity*.
542 Front Immunol, 2017. **8**: p. 1454.
- 543 10. Duewell, P., et al., *NLRP3 inflammasomes are required for atherogenesis and activated by*
544 *cholesterol crystals*. Nature, 2010. **464**(7293): p. 1357-61.
- 545 11. Broderick, L., et al., *The inflammasomes and autoinflammatory syndromes*. Annu Rev Pathol,
546 2015. **10**: p. 395-424.
- 547 12. Schmid-Burgk, J.L., et al., *A Genome-wide CRISPR (Clustered Regularly Interspaced Short*
548 *Palindromic Repeats) Screen Identifies NEK7 as an Essential Component of NLRP3*
549 *Inflammasome Activation*. J Biol Chem, 2016. **291**(1): p. 103-9.
- 550 13. Ito, M., et al., *Bruton's tyrosine kinase is essential for NLRP3 inflammasome activation and*
551 *contributes to ischaemic brain injury*. Nat Commun, 2015. **6**: p. 7360.
- 552 14. Tapia-Abellan, A., et al., *MCC950 closes the active conformation of NLRP3 to an inactive*
553 *state*. Nat Chem Biol, 2019. **15**(6): p. 560-564.
- 554 15. Mayor, A., et al., *A crucial function of SGT1 and HSP90 in inflammasome activity links*
555 *mammalian and plant innate immune responses*. Nat Immunol, 2007. **8**(5): p. 497-503.
- 556 16. Stutz, A., et al., *ASC speck formation as a readout for inflammasome activation*. Methods Mol
557 Biol, 2013. **1040**: p. 91-101.
- 558 17. Li, Z., et al., *Phosphatidylinositol 3-kinase-gamma activates Bruton's tyrosine kinase in*
559 *concert with Src family kinases*. Proc Natl Acad Sci U S A, 1997. **94**(25): p. 13820-5.
- 560 18. Wang, H., et al., *A frequent hypofunctional IRAK2 variant is associated with reduced*
561 *spontaneous hepatitis C virus clearance*. Hepatology, 2015. **62**(5): p. 1375-1387.
- 562 19. Khan, W.N., et al., *Defective B cell development and function in Btk-deficient mice*. Immunity,
563 1995. **3**(3): p. 283-99.
- 564 20. Khare, S., et al., *Measuring NLR Oligomerization I: Size Exclusion Chromatography, Co-*
565 *immunoprecipitation, and Cross-Linking*. Methods Mol Biol, 2016. **1417**: p. 131-43.
- 566 21. Hornung, V., et al., *Silica crystals and aluminum salts activate the NALP3 inflammasome*
567 *through phagosomal destabilization*. Nat Immunol, 2008. **9**(8): p. 847-56.
- 568 22. Warnecke, A., et al., *PyTMs: a useful PyMOL plugin for modeling common post-translational*
569 *modifications*. BMC Bioinformatics, 2014. **15**: p. 370.
- 570 23. Mackerell, A.D., *Developments in the CHARMM all-atom empirical energy function for*
571 *biological molecules*. Abstracts of Papers of the American Chemical Society, 1998. **216**: p.
572 U696-U696.

- 573 24. Jo, S., et al., *CHARMM-GUI: a web-based graphical user interface for CHARMM*. J Comput
574 Chem, 2008. **29**(11): p. 1859-65.
- 575 25. Jo, S., et al., *PBEQ-Solver for online visualization of electrostatic potential of biomolecules*.
576 Nucleic Acids Res, 2008. **36**(Web Server issue): p. W270-5.

577

578

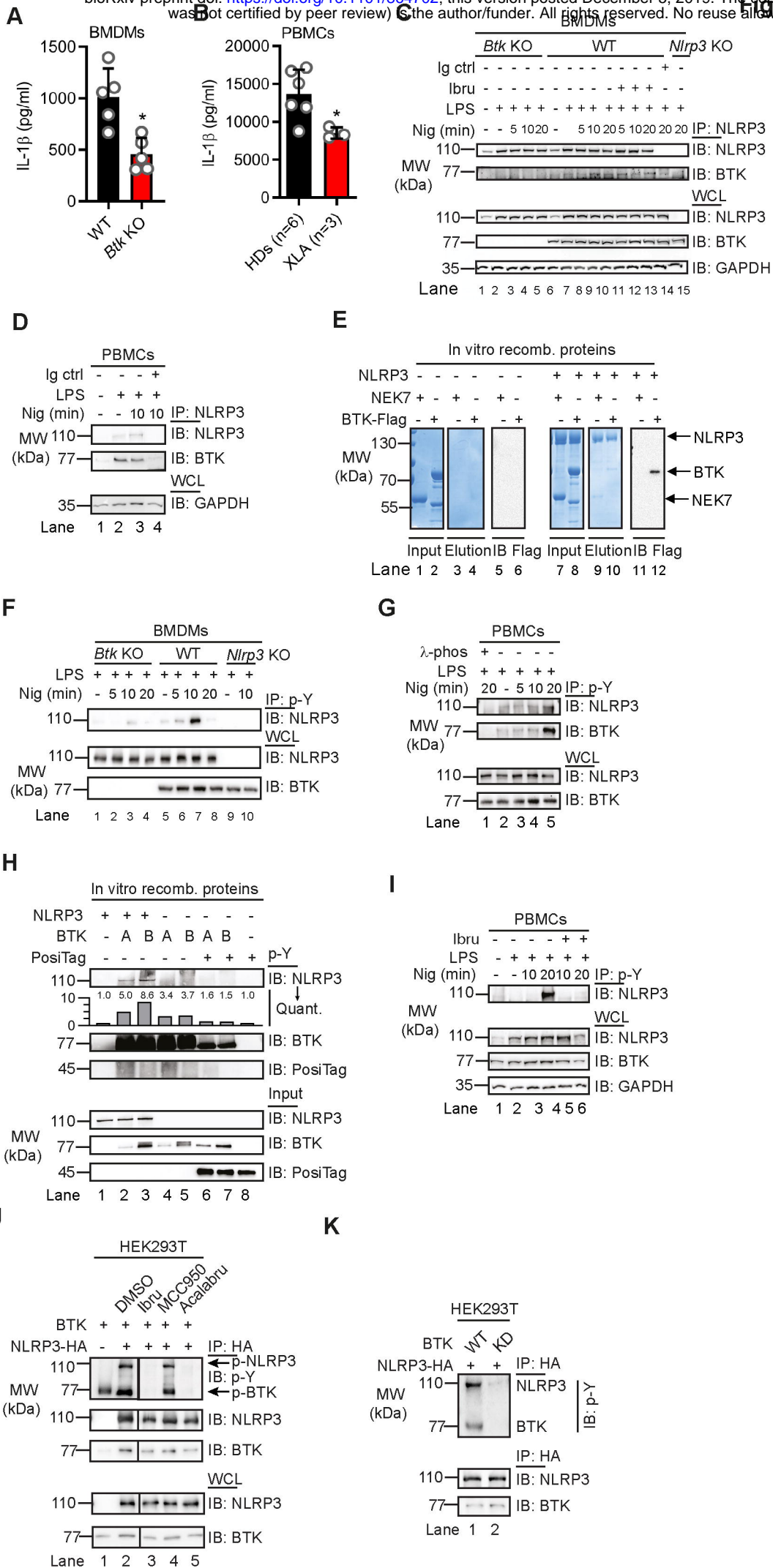


Figure 1

